Research paper

Monitoring the Vegetation Dynamics of Early Succession Following a Landslide on Shanping Forest Road

Fu-Shan Chou,[1)] Wen-Chih Lin,[1)] Yung-Hsiu Chen,[1)] Chun-Kuei Liao[2,3)]

【Summary】

The purpose of this study was to monitor the vegetation dynamics of a landslide on Shanping Forest Road (at 5.3 Km) using a wireless sensor network system and field floristic surveys between 2011 and 2013. In April 2011, 3 dynamic plots (20×20 m) were demarcated on the landslide. At the center of each quadrate, a small quadrate (1×1 m) was demarcated to survey understory plants. All live woody stems with a diameter at breast height (dbh) of ≧1 cm in the dynamic plots were identified and grouped into relevant species, measured for dbh and canopy crown, and mapped onto an X-Y coordinate position. Floristic surveys were conducted in April and October of every year for dry and rainy season data, respectively. Image J software was used to analyze vegetation photographs to estimate the vegetation cover of the landslide area. Importance value (IV) parameters were used to describe the population structure of the plants. Proportions of vegetation that covered the landslide area were 6.86% (Apr. 2011), 17.96% (Otc. 2011), 14.68% (Apr. 2012), 30.5% (Otc. 2012), 15.9% (Apr. 2013), and 33.4% (Otc. 2013). The proportion of vegetation gradually increased each year, and a conspicuous difference existed in the amount of vegetation between the dry and rainy seasons. The forest canopy surrounding the landslide was dominated by pioneer trees such as *Trema orientalis*, *Mallotus paniculatus*, *Macaranga tanarius*, *Hibiscus taiwanensis*, and *Rhus javanica*. Their IVs did not gradually increase each years and a conspicuous difference existed in the amount of vegetation between the dry and rainy seasons. The IV dynamics of *Mikania micrantha* gradually decreased each year. In contrast, the IVs of *Bidens*. *pilosa* increased each year.

Key words: Shanping Forest Road, landslide, vegetation dynamics.

Chou FS, Lin WC, Chen YH, Liao CK. 2015. Monitoring the vegetation dynamics of early succession following a landslide on Shanping Forest Road. Taiwan J For Sci 30(4):217-28.

[1)] Liouguei Research Center, Taiwan Forestry Research Institute, 198 Chunghsing Village, Liouguei District, Kaohsiung City 84443, Taiwan. 林業試驗所六龜研究中心，84443高雄市六龜區中興村198號。

[2)] Department of Biological Science, National Sun Yat-sen Univ., 70 Lianhai Rd., Kaohsiung 80424, Taiwan. 國立中山大學生物科學系，80424高雄市蓮海路70號。

[3)] Corresponding author, e-mail:chunkuei.liao@gmail.com 通訊作者。

Received April 2015, Accepted July 2015. 2015年4月送審 2015年7月通過。

研究報告

扇平林道崩塌地演替初期植被動態之監測

周富三[1)] 林文智[1)] 陳永修[1)] 廖俊奎[2,3)]

摘　要

本研究的目的是使用無線感應網路系統及野外植相調查來監測2011至2013年扇平林道5.3 K處崩塌地的植群動態。在崩塌地內設置3個20 m×20 m的永久樣區，記錄樣區內所有的樹木名稱，胸高直徑達1 cm以上者測量其胸高直徑，胸高直徑未達1 cm以上者則測量其地徑，並測量樹高、冠幅及每木位置，每年的4及10月各調查一次，分別代表乾溼季的資料。植被覆蓋度是用生物影像處理分析軟體Image J分析植被照片而得，植物介量採用重要值指數來計算。結果顯示扇平林道5.3 K處崩塌地植被覆蓋面積有逐年增加的趨勢且乾溼季有顯著差異，植被覆蓋面積佔總崩塌地面積的比例分別為6.86% (2011/4), 17.96% (2011/10), 14.68% (2012/4), 30.5% (2012/10), 15.9% (2013/4), 33.4% (2013/10)。崩塌地內主要的樹木組成，以山黃麻、白匏子、血桐、山芙蓉及羅氏鹽膚木等陽性先驅樹種為優勢，這些樹木的重要值並沒有逐年增加的趨勢且乾溼季的重要值無顯著差異。小花蔓澤蘭的重要值有逐年下降的趨勢，而大花咸豐草的重要值則有逐年增加的趨勢。

關鍵詞：扇平林道、崩塌地、植被動態。

周富三、林文智、陳永修、廖俊奎。2015。扇平林道崩塌地演替初期植被動態之監測。台灣林業科學 30(4):217-28。

INTRODUCTION

Landslides are movements of the earth's surface, and in Taiwan they are typically triggered by rainfall events and earthquakes. On 8 August 2009, typhoon Morakot induced catastrophic amounts of rainfall, triggering enormous landslides in southern Taiwan. To clarify the factors that caused the devastating Shiaolin Village landslide, Tsou et al. (2011) investigated the geological and geomorphological features of the surrounding area. Results of that investigation indicated that the geological structure, cumulative rainfall, and gravitational deformation of the area were the primary factors that caused the landslide. The Liukuei Experimental Forest (LEF), which is managed by the Taiwan Forestry Research Institute, was located in the peak rainfall regions and severe landslides and road destruction occurred in this area. Following Typhoon Morakot, Lu et al. (2011) adopted a statistical approach to study spatial relation, between landslides and their geographic factors in the LEF. Results indicated that extremely heavy rainfall primarily triggered the landslides during the typhoon. In all, 204 locations experienced identifiable landslides, spanning an area of approximately 804.49 ha. Steepness, aspects, and distances to roads and streams contributed to slope instability. In addition, 34 landslides (24.7% of the landslides area) occurred within 50 m of a forest road, each of which occupied an average area of 5.79 ha. This indicated that the landslides in the LEF were closely related to forest road construction.

Various techniques have been used to compile landslide event-inventory maps such as interpreting aerial and satellite images (Mackey and Tudor 2000, Townsend and Walsh 2001, Fiorucci et al. 2011), digitally analyzing high-resolution digital elevation models (DEMs) obtained from airborne Lidar sensors (McKeana and Roering 2004, Ardizzone et al. 2007, Kasai et al. 2009), and conducting reconnaissance field surveys (Dapporto et al. 2005, Cardinali et al. 2006, Santangelo et al. 2010). A wireless sensor network system was established in the ecological and scientific gardens of the Shanping Forest in 2006. This system was installed to study the animal soundscape (Chen et al. 2012, Hsieh et al. 2012) and bee behavior (Lu et al. 2009). The purpose of this study was to monitor vegetation dynamics following a landslide on Shanping Forest Road (at 5.3 Km) using a wireless sensor network system and field floristic surveys to elucidate the early successional process of the landslide.

MATERIALS AND METHODS

Study site

On 8 August 2009, Typhoon Morakot caused an approximately 6.67-ha landslide (2541177.10N, 216429.43E, TWD 97) near 5.3 km of Shanping Forest Road (Fig. 1). The approximate elevation of this landslide rangs 500~600 m. Its aspect and average slope were 143° and 30°, respectively. Based on recordings from the Shanping meteorological station, the average annual temperature and precipitation in this area are approximately 20.6℃ and 3500 mm, respectively. Approximately 80% of the annual rainfall occursduring the summer season between May and September. The dry season is from November to April. The rainy and dry seasons are fairly clear (Lu et al. 2011). After natural succession occurred, plants colonized the landslide; currently, the landslide area contains a mosaic of plants.

Methods

Monitoring the vegetation coverage and landslide area dynamics

To monitor the vegetation coverage and dynamics of the landslide area, we installed a 6-m-high iron tower at the ecological and scientific garden of Shanping Forest, with an automatic camera mounted at the top. We configured the camera to capture a photograph at 10:00 daily and sent this photograph to a computer at a work station through the wireless sensing network system for a vegetation coverage analysis.

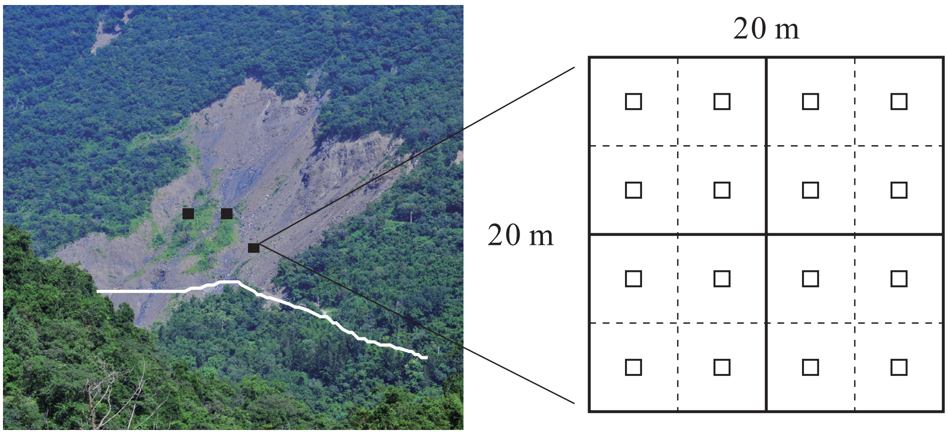

Fig. 1. Photo of the study area by camera showing the plot location and plot sketch map.

Floristic surveys

In April 2011, 3 plots (20×20 m) were demarcated on the landslide. Each dynamic plot was divided into 16 quadrates (25 m^2 per quadrate) (Fig. 1). All live woody stems with a diameter at breast height (dbh) of ≧1 cm in the dynamic plots were identified and grouped into relevant species, measured for dbh and canopy crown, mapped onto an X-Y coordinate position, and numbered using aluminum identification tags. At the center of each quadrate (5×5 m), a small quadrate (1×1 m) was demarcated to survey understory plants. All live plants in the small quadrates were identified and grouped into relevant species, estimations were made regarding plant cover, and the frequency of plant occurrence was measured using a wooden frame (1×1 m), dividing 100 subquadrates (10×10 cm) using cotton thread. The dynamic plots were sequentially measured in April and October of every year. The scientific names of the plants were labeled according to the *Flora of Taiwan* (Huang et al. 2003).

Statistical analysis

Image J (vers. 1.44) software, which is an image processing program developed at the National Institute of Health, was used to calculate the vegetation cover of the landslide. Differences in the vegetation covering the landslide between the dry and rainy seasons were analyzed at a 5% significance level by paired *t*-test procedures Statistical Product and Service Solutions (SPSS 17.0, Chicago I.L, USA). IV of the parameters were used to describe the population structure of the plants for overstory communities. An IV was calculated for all trees of each plot, as (relative density + relative dominance) / 2 (Curtis and McIntosh 1950). The density was determined based on the number of individual trees per plot. Dominance was determined based on the area covered by individual trees. For understory communities, another IV was calculated for all plants of each quadrate, equaling (relative coverage + relative frequency) / 2 (Curtis and McIntosh 1950). The coverage was typically defined as the vertical projection of the crown of a species onto the ground surface. The frequency was determined based on the number of times the cotton thread intersected a species.

RESULTS AND DISCUSSION

Dynamics of vegetation coverage

During the survey period, landslide photographs were taken with an automatic camera (Fig. 2). Proportions of vegetation cover on the landslide were 6.86% (Apr. 2011), 17.96% (Oct. 2011), 14.68% (Apr. 2012), 30.5% (Oct. 2012), 15.9% (Apr. 2013), and 33.4% (Otc. 2013) (Fig. 3). The results indicated that the proportions of vegetation cover gradually increased each year, demonstrating a conspicuous difference ($p = 0.002$) between the dry and rainy seasons.

After Typhoon Morakot, the landslide did not cause any catastrophic events, and the arrival of various plants increased the diversity of species and cover of certain species on the landslide. Natural succession occurred on the landslide; therefore, the proportion of vegetation cover on the landslide gradually increased over time. Seasonal variations of the physical environment, temperature, and precipitation particularly affected plant growth. In the dry season, when there were a relatively low temperature and little precipitation, the growth of plants was slow, but in the rainy season, when there were a relatively high temperature and abundant precipitation, plant growth was comparatively rapid. Results indicated a conspicuous difference in proportions of vegetation coverage on the landslide between the dry and rainy seasons.

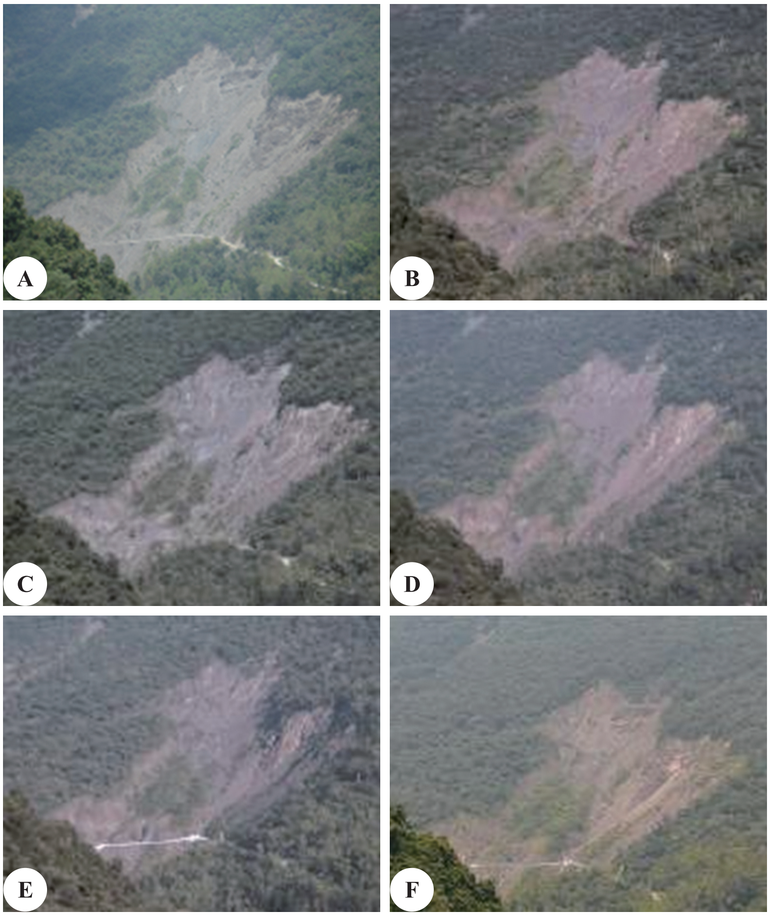

Fig. 2. Photographs of the landslide taken with an automatic camera. A: (Apr. 2011), B: (Otc. 2011), C: (Apr. 2012), D: (Otc. 2012), E: (Apr. 2013), F: (Otc. 2013).

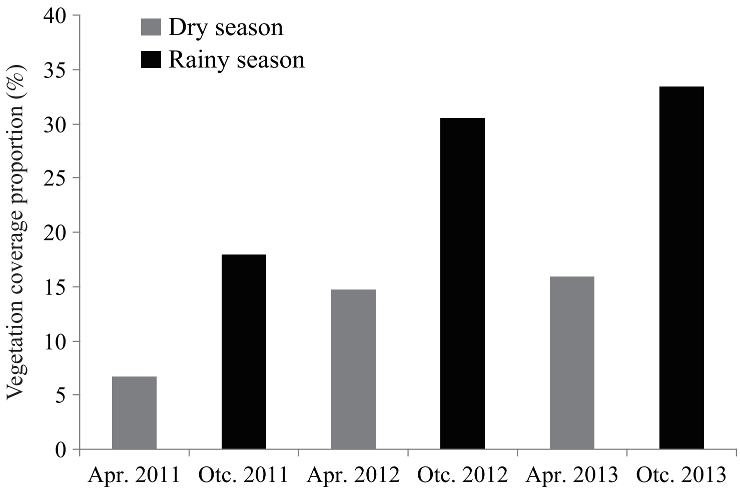

Fig. 3. Vegetation coverage proportion dynamics of the landslide.

Floristic composition

The landslide was primarily dominated by pioneer trees (*Trema orientalis*, *Mallotus paniculatus*, *Macaranga tanarius*, *Hibiscus taiwanensis*, and *Rhus javanica*). Table 1 shows the tree compositions and IV dynamics in permanent plots of the landslide. Figure 4 shows that the IV dynamics of dominant trees did not gradually increase each year, and there were no conspicuous differences ($p = 0.452$, $p = 0.237$, $p = 0.385$, $p = 0.211$, $p = 0.926$) between the dry and rainy seasons at a 5% significance level by paired *t*-test procedures. Table 2 shows understory plants and IV dynamics in permanent plots of the landslide. Figure 5 shows the IV dynamics of *Mikania micrantha* and *Bidens pilosa*, indicating that *Mi. micrantha* gradually increased each year. In contrast, the IVs of *B. pilosa* decreased each year.

During 2011~2013, the landslide was primarily dominated by *T. orientalis*, *Mal. paniculatus*, *Mac. tanarius*, *H. taiwanensis*, and *R. javanica*, yielding a total IV of 80.76%. These pioneer trees grow rapidly and display shade-intolerant characteristics; the closing canopy offered a suitable microenvironment for shade-tolerant trees (Whitmore 1989), and their root systems can firmly grasp soil and stone stabilizing the landslide (Greenway 1987). Lin et al. (2012) developed a 2D numerical model of the soil-root system of *T. orientalis* to correlate the shear strength increment due to roots. Next, Lin et al. (2013) proposed a 3D mechanical conversion model for the soil-root system of *T. orientalis* to evaluate the contribution of the root system to the stability of a slope. Their results confirmed that root systems of *T. orientalis* can firmly grasp soil and stone promoting the stability of a landslide. Therefore, we suggest that these pioneer trees can offer the materials required for the forest recovery in this landslide-affected region. Although the landslide was primarily dominated by these pioneer trees at present, there are many shade-tolerant trees (*Litsea hypophaea*, *Machilus japonica*, *Machilus zuihoensis*, *Castanopsis formosana*) that have appeared in the understory (Table 1). We presume that the landslide will eventually be restored to a typical lower montane evergreen broadleaf forest in Taiwan, dominated by Lauraceae and Fagaceae plants, through a natural succession process.

The ecological niche of an organism depends not only on where it lives but also on what it does, as described by Odum and Odum (1959). These pioneer trees can also locally coexist due to processes other than simple niche separation, namely due to stochastic spatiotemporal population dynamics. In the early succession process of the landslide, IV were preoccupied more niches than could dominate in the habitat. Therefore, the IV dynamics of dominant trees have not gradually increased each year, and there are no conspicuous differences between the dry and rainy seasons.

The understory of the landslide was dominated by *Mi. micrantha* and *B. pilosa*, which are naturalized plants. The IVs of *Mi. micrantha* decreased from 28.2% (2011) to 6.09% (2013). We reasoned that *Mi. micrantha* is a vine, and its coverage and frequency in the small quadrates may have been underestimated when leaves of *Mi. micrantha* climbing on the tall canopies of overstory trees were not assessed. Furthermore, *Mi. micrantha* blooms in October, bears fruit in December, yields a substantial amount of seeds, and then withers. The IVs of *B. pilosa* increased from 12.12% (2011) to 32.81% (2013). *Bidens pilosa* has good acclimatization and has become a serious invasive plant in Taiwan. Huang et al. (2012) studied the floral biology of *B. pilosa* including the floral structure, the process of

Table 1. Dynamics of importance values (IVs) of trees (individuals with a diameter at breast height of ≧ 1 cm) in the landslide permanent plots. Rde, relative density; Rdo, relative dominance

Species	Apr. 2011			Otc. 2011			Apr. 2012			Otc. 2012			Apr. 2013			Otc. 2013		
	Rde	Rdo	IV	Rde	Rdo	IV	Rde	Rdo	IV	Rde	Rdo	IV	Rde	Rdo	IV	Rde	Rdo	IV
Trema orientalis	2.1	55.2	38.7	17.8	52.2	35.0	16.0	53.7	34.8	14.9	54.9	34.9	14.2	48.7	31.5	13.5	41.3	27.4
Mallotus paniculatus	21.5	6.7	14.1	27.9	7.2	17.6	29.0	6.4	17.7	29.1	8.0	18.5	29.7	8.4	19.1	27.9	11.0	19.4
Macaranga tanarius	12.1	7.7	9.9	9.5	10.6	10.0	8.4	12.0	10.2	7.7	14.4	11.1	8.0	16.6	12.3	7.2	18.3	12.8
Hibiscus taiwanensis	10.7	9.0	9.9	10.0	6.2	8.1	9.8	7.6	8.7	8.7	5.5	7.1	8.8	7.4	8.1	7.7	6.3	7.0
Rhus javanica	12.6	4.8	8.7	12.1	9.8	10.9	13.2	8.5	10.8	16.2	8.1	12.1	14.8	7.7	11.3	17.5	11.0	14.3
Metapetrocomea peltata	3.0	2.6	2.8	2.8	0.8	1.8	3.2	1.1	2.1	3.4	0.6	2.0	4.0	1.3	2.6	3.9	1.3	2.6
Trema cannabina	2.5	2.0	2.2	1.7	1.3	1.5	1.5	1.1	1.3	1.3	0.8	1.0	1.2	0.8	1.0	0.9	0.5	0.7
Dendrocnide meyeniana	2.0	1.0	1.5	1.6	0.8	1.2	1.4	0.4	0.9	1.1	0.7	0.9	0.4	0.1	0.3	0.7	0.4	0.6
Pouzolzia elegans	0.7	2.2	1.4	0.7	2.0	1.4	0.6	1.4	1.0	0.9	0.6	0.7	0.8	1.7	1.3	0.7	0.9	0.8
Mallotus philippensis	0.7	2.1	1.4	0.8	1.4	1.1	0.8	0.9	0.9	0.9	0.4	0.6	1.5	1.2	1.3	1.4	1.5	1.5
Coffea arabica	2.0	0.8	1.4	1.8	0.5	1.2	2.0	0.3	1.2	2.0	0.3	1.1	2.1	0.3	1.2	2.4	0.4	1.4
Ardisia cornudentata	1.8	0.4	1.1	3.4	0.4	1.9	3.9	0.6	2.2	4.0	0.6	2.3	4.7	0.8	2.7	4.9	0.9	2.9
Tetradium glabrifolium	1.8	0.3	1.1	1.3	0.4	0.9	1.1	0.4	0.8	0.9	0.2	0.6	0.8	0.3	0.6	0.7	0.6	0.6
Glochidion rubrum	1.3	0.2	0.7	1.6	0.3	1.0	2.1	0.4	1.3	2.4	0.5	1.5	2.6	0.5	1.5	3.8	0.9	2.4
Sapium discolor	1.0	0.5	0.7	1.0	1.5	1.2	1.0	1.1	1.0	0.5	0.8	0.7	0.5	0.6	0.5	0.4	0.3	0.3
Diospyros eriantha	0.3	0.9	0.6	0.3	1.8	1.0	0.3	1.3	0.8	0.3	0.9	0.6	0.3	0.7	0.5	0.3	0.7	0.5
Buddleja asiatica	0.1	0.9	0.5	0.1	0.3	0.2	0.1	0.4	0.2	0.1	0.3	0.2						
Champereia manillana	0.1	0.8	0.4	0.1	0.4	0.3	0.1	0.0	0.1	0.2	0.1	0.1	0.2	0.1	0.1	0.3	0.2	0.2
Zanthoxylum ailanthoides	0.5	0.2	0.3	0.4	0.3	0.3	0.4	0.2	0.3	0.4	0.1	0.2	0.2	0.0	0.1	0.2	0.1	0.1
Anthocephalus chinensis	0.4	0.3	0.3	0.3	0.5	0.4	0.2	0.5	0.4	0.1	0.0	0.0	0.1	0.0	0.1	0.2	0.3	0.3
Leea guineensis	0.2	0.3	0.2	0.1	0.0	0.1	0.1	0.0	0.1	0.3	0.1	0.2	0.2	0.1	0.2	0.3	0.2	0.3
Aleurites montana	0.4	0.1	0.2	0.4	0.1	0.3	0.4	0.1	0.2	0.4	0.2	0.3	0.3	0.2	0.3	0.4	0.6	0.5
Sapindus mukorossii	0.2	0.2	0.2	0.2	0.1	0.2	0.2	0.2	0.2	0.2	0.1	0.2	0.2	0.2	0.2	0.2	0.2	0.2
Litsea hypophaea	0.3	0.1	0.2	0.2	0.1	0.2	0.2	0.2	0.2	0.2	0.1	0.2	0.2	0.2	0.2	0.3	0.2	0.3
Machilus japonica	0.2	0.1	0.1	0.2	0.1	0.1	0.2	0.1	0.1	0.2	0.0	0.1	0.3	0.0	0.2	0.3	0.0	0.2
Maesa perlaria	0.2	0.1	0.1	0.6	0.2	0.4	0.6	0.1	0.4	0.6	0.2	0.4	0.7	0.3	0.5	0.7	0.4	0.5
Ficus septica	0.2	0.1	0.1	0.4	0.1	0.2	0.4	0.4	0.4	0.3	0.1	0.2	0.4	0.5	0.4	0.4	0.4	0.4
Meliosma rhoifolia	0.2	0.1	0.1	0.1	0.0	0.1	0.2	0.0	0.1	0.2	0.1	0.1	0.1	0.0	0.0	0.2	0.1	0.1
Callicarpa formosana	0.2	0.1	0.1	1.0	0.1	0.6	1.0	0.1	0.6	0.9	0.1	0.5	0.9	0.1	0.5	0.9	0.2	0.5
Acacia confusa	0.2	0.0	0.1	0.1	0.0	0.0	0.2	0.0	0.1	0.2	0.0	0.1	0.2	0.1	0.2	0.3	0.2	0.2
Fraxinus griffithii	0.1	0.1	0.1	0.1	0.1	0.1	0.1	0.0	0.1	0.1	0.0	0.1	0.1	0.0	0.1	0.1	0.1	0.1
Lagerstroemia subcostata	0.1	0.0	0.1	0.1	0.0	0.0	0.1	0.0	0.1	0.1	0.1	0.1	0.1	0.1	0.1	0.1	0.1	0.1
Aphananthe aspera	0.1	0.0	0.1	0.2	0.0	0.1	0.1	0.0	0.0	0.2	0.0	0.1	0.2	0.0	0.1	0.3	0.1	0.2
Glycosmis citrifolia	0.1	0.0	0.1	0.1	0.0	0.0	0.2	0.0	0.1	0.1	0.0	0.0	0.2	0.0	0.1	0.2	0.0	0.1
Elaeocarpus sylvestris	0.1	0.0	0.1	0.1	0.0	0.0	0.1	0.0	0.0	0.1	0.0	0.0	0.1	0.0	0.1	0.1	0.1	0.1
Machilus zuihoensis	0.1	0.0	0.1	0.1	0.0	0.0	0.1	0.0	0.0							0.1	0.0	0.0
Murraya paniculata				0.1	0.1	0.1	0.2	0.0	0.1	0.2	0.1	0.1	0.2	0.1	0.1	0.2	0.1	0.1
Mallotus japonicus				0.1	0.0	0.1	0.1	0.1	0.1	0.2	0.1	0.1	0.2	0.1	0.1	0.1	0.1	0.1
Ficus nervosa				0.1	0.0	0.0												
Bridelia tomentosa				0.1	0.0	0.0	0.1	0.0	0.0	0.1	0.0	0.1	0.1	0.0	0.1	0.1	0.1	0.1
Wendlandia formosana				0.1	0.0	0.0	0.1	0.0	0.0									
Phyllanthus multiflorus				0.1	0.0	0.0	0.1	0.0	0.0	0.2	0.0	0.1	0.1	0.0	0.0	0.1	0.0	0.1
Koelreuteria henryi				0.1	0.0	0.0	0.2	0.0	0.1	0.1	0.0	0.0	0.1	0.0	0.0	0.1	0.0	0.0
Rhus succedanea							0.1	0.0	0.0									
Ficus irisana							0.1	0.0	0.0									
Croton cascarilloides							0.1	0.0	0.0									
Castanopsis formosana																0.2	0.2	0.2
Cinchona pubescens										0.2	0.8	0.5	0.2	0.5	0.4	0.2	0.2	0.2

secondary pollen presentation, and the pollen/ovule ratio. They found significant differences in the number of disk florets per capitulum (range 19~61, average 44.1) and the number of pollen grains in each floret (range 6556~11,378) among individuals. Secondary pollen presentation was observed as the growing style brushes and pumps pollen grains out of the anther tube. Incomplete protandry was found from the observation of the flower-

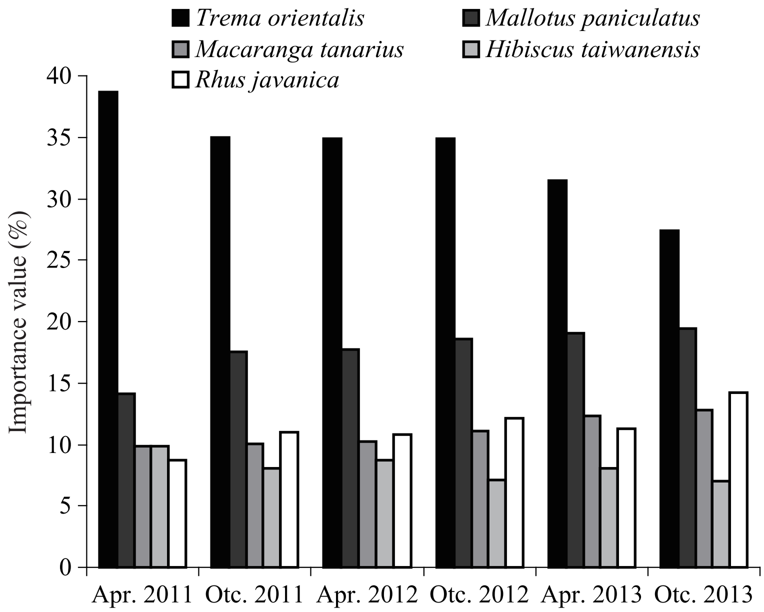

Fig. 4. Dynamics of important values of dominant trees.

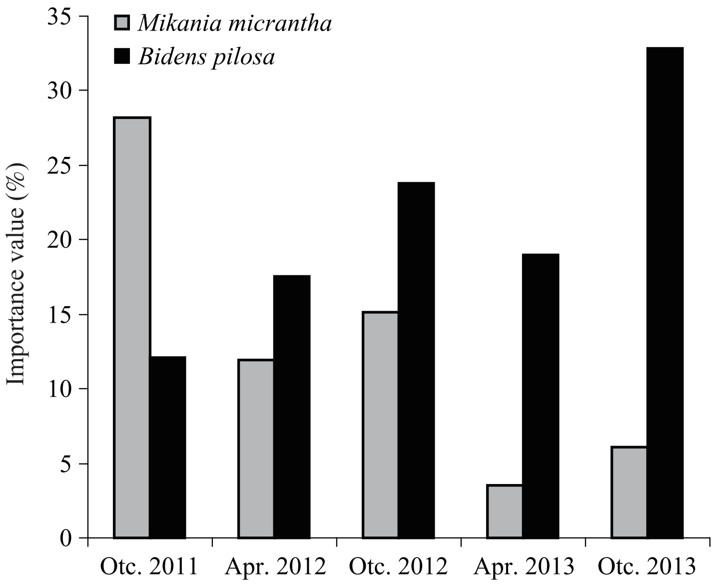

Fig. 5. Dynamics of important values of *Mikania micrantha* and *Bidens pilosa*.

Table 2. Understory plants and importance value dynamics in permanent plots of the landslide. Rco, relative coverage; Rfe, relative frequency

Species	Otc. 2011			Apr. 2012			Otc. 2012			Apr. 2013			Otc. 2013		
	Rco	Rfr	IV	Rco	Rfr	IV	Rco	Rfr	IV	Rco	Rfr	IV	Rco	Rfr	IV
Mikania micrantha	29.7	26.7	28.2	10.4	13.5	11.9	15.0	15.4	15.2	2.8	4.3	3.5	5.1	7.1	6.1
Bidens pilosa	12.8	11.4	12.1	17.5	17.5	17.5	26.1	21.5	23.8	18.9	19.0	19.0	36.3	29.3	32.8
Rhus javanica	6.8	4.8	5.8	7.8	5.6	6.7	8.5	6.7	7.6	5.2	3.8	4.5	7.4	6.5	7.0
Pueraria montana	5.7	5.5	5.6	4.3	5.4	4.9	4.0	4.2	4.1	6.9	7.2	7.1	2.5	3.2	2.9
Ipomoea indica	4.9	5.3	5.1	1.9	1.9	1.9	1.0	1.5	1.2	1.0	1.0	1.0	1.0	1.6	1.3
Blumea balsamifera	5.2	4.0	4.6	7.5	6.6	7.0	3.7	2.4	3.0	6.5	4.2	5.4	0.7	1.0	0.8
Microlepia speluncae	3.1	3.9	3.5	2.4	3.0	2.7	3.5	3.7	3.6	3.2	2.6	2.9	1.4	1.7	1.5
Blumea riparia	2.5	3.8	3.1	1.7	1.7	1.7	1.0	1.2	1.1	0.3	0.5	0.4	0.2	0.3	0.2
Cyclosorus parasiticus	3.1	2.2	2.6	2.9	2.1	2.5	1.4	1.4	1.4	4.0	3.2	3.6	2.5	2.2	2.3
Mallotus paniculatus	2.3	2.8	2.6	2.6	2.1	2.4	2.0	2.2	2.1	2.4	1.8	2.1	1.0	0.9	0.9
Chromolaena odorata	2.1	2.6	2.4	3.0	3.3	3.2	8.0	8.0	8.0	5.6	6.0	5.8	8.7	8.9	8.8
Trema orientalis	2.0	2.3	2.2	1.5	2.1	1.8	4.1	2.9	3.5	1.0	0.7	0.8			
Hiptage benghalensis	2.0	2.0	2.0	1.5	1.3	1.4	0.2	0.3	0.3	0.8	1.3	1.1	1.3	0.9	1.1
Polygonum multiflorum	1.5	2.3	1.9	1.5	1.8	1.6	0.4	0.4	0.4	1.5	1.7	1.6	0.7	1.1	0.9
Pityrogramma calomelanos	1.6	1.9	1.8	2.7	2.1	2.4	2.1	1.9	2.0	1.9	1.6	1.8	0.5	0.8	0.7
Cyrtococcum accrescens	1.1	2.3	1.7	0.4	0.6	0.5	0.6	1.5	1.0	2.3	2.1	2.2	1.7	2.4	2.0
Dendrocnide meyeniana	1.6	1.7	1.6	0.6	0.4	0.5	0.2	0.2	0.2	0.0	0.0	0.0			
Rhynchelytrum repens	1.3	1.4	1.4	2.6	3.0	2.8	0.2	1.3	0.8	0.3	1.1	0.7	0.3	1.1	0.7
Elephantopus mollis	1.1	1.2	1.1	0.4	0.5	0.4	1.1	1.1	1.1	0.2	0.3	0.3	1.2	1.1	1.1
Pouzolzia elegans	0.8	1.2	1.0	2.6	2.5	2.5	2.3	1.9	2.1	3.7	4.5	4.1	4.2	2.8	3.5
Microstegium ciliatum	0.6	1.1	0.8	5.9	6.3	6.1	3.5	4.5	4.0	2.3	3.5	2.9	0.7	0.8	0.7
Paspalum conjugatum	0.4	0.9	0.7	0.8	1.2	1.0	0.7	1.5	1.1	2.4	3.1	2.8	1.3	2.5	1.9
Pteris tokioi	0.7	0.6	0.7	1.0	0.7	0.8	0.4	0.4	0.4	0.8	0.9	0.9	0.1	0.1	0.1
Mallotus philippensis	0.6	0.7	0.7	2.7	2.3	2.5	2.1	1.8	1.9	4.4	2.8	3.6	2.8	1.7	2.2
Metapetrocomea peltata	0.6	0.7	0.6	1.3	1.1	1.2	0.8	1.3	1.1	4.1	3.9	4.0	1.1	1.2	1.1
Nephrolepis auriculata	0.6	0.6	0.6	2.6	1.4	2.0	0.9	1.2	1.0	5.4	4.2	4.8	5.0	5.2	5.1
Phyllanthus multiflorus	0.3	0.8	0.6	0.4	0.4	0.4	0.2	0.2	0.2	0.6	0.6	0.6	0.4	0.5	0.5
Deeringia amaranthoides	0.5	0.6	0.5	0.3	0.4	0.3				0.0	0.0	0.0			
Lygodium japonicum	0.4	0.6	0.5	0.4	0.4	0.4	0.8	1.6	1.2	0.8	1.7	1.2	0.7	1.3	1.0
Pteris vittata	0.3	0.7	0.5	0.8	0.9	0.9	0.1	0.2	0.2	0.5	0.6	0.5	0.4	0.6	0.5
Hibiscus taiwanensis	0.5	0.4	0.5	1.5	1.5	1.5	0.6	0.6	0.6	0.7	0.7	0.7			
Macaranga tanarius	0.5	0.5	0.5	0.6	0.4	0.5	0.2	0.3	0.3	0.0	0.0	0.0			
Aleurites montana	0.3	0.3	0.3	0.0	0.0	0.0				0.0	0.0	0.0			
Merremia gemella	0.2	0.2	0.2	0.1	0.1	0.1	0.3	0.4	0.3	0.3	0.4	0.3	0.5	0.5	0.5
Oplismenus compositus	0.2	0.2	0.2	0.7	0.5	0.6	0.2	0.5	0.3	0.6	0.6	0.6	0.7	1.2	0.9
Diplocyclos palmatus	0.2	0.2	0.2							0.0	0.0	0.0			
Crassocephalum crepidioides	0.2	0.1	0.1	0.1	0.1	0.1	0.1	0.1	0.1	0.0	0.0	0.0	0.2	0.1	0.2
Passiflora suberosa	0.1	0.2	0.1	0.2	0.2	0.2	0.0	0.1	0.1	0.2	0.3	0.2	0.1	0.1	0.1
Boehmeria pilosiuscula	0.1	0.2	0.1	0.1	0.1	0.1	0.1	0.1	0.1	0.0	0.0	0.0			
Pouzolzia zeylanica	0.1	0.2	0.1							0.0	0.0	0.0			
Synedrella nodiflora	0.1	0.1	0.1							0.0	0.0	0.0	0.0	0.0	0.0
Maesa perlaria	0.1	0.1	0.1				0.0	0.0	0.0	0.1	0.0	0.1	0.1	0.1	0.1
Mussaenda pubescens	0.1	0.1	0.1				0.0	0.1	0.1	0.2	0.2	0.2	0.2	0.3	0.3
Miscanthus floridulus	0.1	0.1	0.1	0.1	0.4	0.3	0.3	0.5	0.4	1.1	2.0	1.6	0.4	0.9	0.7

con't

Diospyros eriantha	0.1	0.1	0.1	0.1	0.1	0.1	0.1	0.1	0.1	0.4	0.5	0.5	0.0	0.0	0.0
Isachne globosa	0.0	0.1	0.1	0.1	0.1	0.1	0.7	1.3	1.0	1.0	1.6	1.3	1.9	2.8	2.3
Clematis grata	0.1	0.0	0.1	0.1	0.0	0.0	0.0	0.1	0.1	0.1	0.0	0.1	0.1	0.3	0.2
Ampelopsis brevipedunculata	0.0	0.1	0.1	0.1	0.1	0.1	0.2	0.4	0.3	0.0	0.0	0.0			
Ageratum conyzoides	0.0	0.1	0.1	0.1	0.1	0.1				0.0	0.0	0.0			
Desmodium sequax	0.0	0.1	0.1	0.0	0.0	0.0				0.0	0.0	0.0			
Pisonia aculeata	0.0	0.1	0.1	0.4	0.7	0.6	0.4	0.7	0.5	0.1	0.0	0.1	0.2	0.2	0.2
Tetradium glabrifolium	0.0	0.1	0.1	0.0	0.0	0.0				0.0	0.0	0.0			
Pseudophegopteris paludosa	0.0	0.0	0.0	0.1	0.1	0.1	0.0	0.1	0.1	0.6	0.5	0.6	0.1	0.1	0.1
Tetrastigma formosanum	0.0	0.0	0.0	0.1	0.2	0.2	0.2	0.2	0.2	0.2	0.1	0.1	0.2	0.3	0.2
Conyza canadensis	0.0	0.0	0.0	0.1	0.1	0.1				0.0	0.0	0.0			
Tricalysia dubia	0.0	0.0	0.0	0.1	0.1	0.1	0.0	0.0	0.0	0.1	0.0	0.1	0.2	0.2	0.2
Onychium siliculosum	0.0	0.0	0.0							0.0	0.0	0.0			
Glochidion rubrum	0.0	0.0	0.0	0.1	0.1	0.1				0.1	0.0	0.1	0.6	0.4	0.5
Callicarpa formosana				0.6	0.5	0.6	0.3	0.3	0.3	0.3	0.3	0.3			
Rubus croceacanthus				0.6	0.5	0.5	0.0	0.1	0.1	0.1	0.2	0.1	0.0	0.0	0.0
Sapindus mukorossii				0.4	0.5	0.4				0.0	0.0	0.0			
Carex baccans				0.1	0.3	0.2	0.1	0.2	0.2	0.3	0.9	0.6	0.8	0.8	0.8
Rhynchosia volubilis				0.2	0.2	0.2	0.2	0.2	0.2	0.4	0.4	0.4	0.1	0.2	0.2
Piper sintenense				0.1	0.2	0.2	0.4	0.4	0.4	0.3	0.5	0.4	1.0	1.2	1.1
Ardisia cornudentata				0.4	0.5	0.4	0.2	0.2	0.2	0.9	0.8	0.9	0.5	0.5	0.5
Malaisia scandens				0.2	0.2	0.2	0.0	0.1	0.1	0.3	0.2	0.3	0.0	0.1	0.1
Glochidion philippicum				0.1	0.1	0.1				0.0	0.0	0.0	0.7	0.5	0.6
Glycosmis citrifolia				0.1	0.1	0.1	0.0	0.0	0.0	0.4	0.9	0.6	0.4	0.4	0.4
Arachniodes aristata				0.1	0.1	0.1	0.1	0.1	0.1	0.1	0.2	0.1	0.1	0.2	0.1
Triumfetta bartramia				0.1	0.1	0.1				0.0	0.0	0.0			
Lycopersicon esculentum				0.1	0.0	0.0				0.0	0.0	0.0			
Cyclosorus taiwanensis							0.1	0.2	0.2	0.0	0.0	0.0			
Pollia miranda							0.0	0.1	0.1	0.0	0.0	0.0	0.0	0.1	0.1
Saccharum spontaneum							0.0	0.1	0.1	0.4	0.3	0.4			
Litsea hypophaea							0.0	0.0	0.0	0.1	0.0	0.1			
Blumea lanceolaria										0.2	0.2	0.2	0.7	0.9	0.8
Jasminum nervosum										0.1	0.0	0.1			
Aphananthe aspera													0.2	0.2	0.2
Liriope minor													0.1	0.0	0.1
Lepidagathis formosensis													0.0	0.1	0.1
Aster indicus													0.0	0.0	0.0

ing process and tests of pollen viability and stigmatic receptivity. A high pollen/ovule ratio (mean±s.e.: 8827±464) was measured which suggested that *B. pilosa* var. *radiata* might be obligately xenogamous. Huang and Kao (2014) compared different breeding systems of 3 varieties of *B. pilosa* in Taiwan to identify what traits make the *radiata* variety invasive in Taiwan. They found that massive achenes produced by sexual reproduction potentially allow the *radiata* variety to disperse into far-reaching habitats. High heterogeneities were found in many traits of the *radiata* variety, which might allow var. *radiata* to have a wide fundamental niche. After becoming established in a new habitat, var. *radiata* can generate many ramets by vegetative reproduction and expand horizontally, eventually occuping the area and becoming dominant. The breeding system and life history traits of var. *radiata*, in combination with the warm and high-light climate and land use changes in Taiwan confer the *radiata* variety advantages over the minor variety. Carol et al. (1998) studied forest regeneration during 2 yr following a recent severe hurricane, and suggested that invasive non-indigenous forest species exhibit the same range of ecological roles as native forest species and compete with native species for particular kinds of regeneration opportunities. Stinson et al. (2006) studied the invasive plant, *Alliaria petiolata*, a European invader of North American forests, and found that it suppresses native plant growth by disrupting mutualistic associations between native canopy tree seedlings and belowground arbuscular mycorrhizal fungi. They elucidated an indirect mechanism by which invasive plants can impact native flora. The IVs of *Mi. micrantha* and *B. pilosa* were quite obviously greater than these of native plants on the landslide. Therefore, we suggest that removing invasive plants at the understory layer would be contributive to accelerating native plant regeneration and succession on the landslide.

ACKNOWLEDGEMENTS

We appreciate the assistance from the Liouguei Research Center, Taiwan Forestry Research Institute during fieldwork. The authors also thank the English editor and 2 anonymous reviewers for kindly improving our manuscript.

LITERATURE CITED

Ardizzone F, Cardinali M, Galli M, Guzzetti F, Reichenbach P. 2007. Identification and mapping of recent rainfall-induced landslides using elevation data collected by airborne Lidar. Nat Haz Earth Syst Sci 7:637-50.

Cardinali M, Galli M, Guzzetti F, Ardizzone F, Reichenbach P, Bartoccini P. 2006. Rainfall induced landslides in December 2004 in south-western Umbria, central Italy: types, extent, damage and risk assessment. Nat Haz Earth Syst Sci 6:237-60.

Chen CC, Chiang PJ, Shieh BS, Lin CC. 2012. Diurnal timing of bird surveys using an acoustic monitoring system in the Shan-Ping Forest Ecological Garden. Taiwan J For Sci 26(4):2-10.

Curtis JT, McIntosh RP. 1950. The interrelations of certain analytic and synthetic phytosociological charaters. Ecology 31:434-55.

Dapporto S, Aleotti P, Casagli N, Polloni G. 2005. Analysis of shallow failures triggered by the 14-16 November 2002 event in the Albaredo valley, Valtellina (northern Italy). Adv Geosciences 2:305-08.

Fiorucci F, Cardinali M, Carlà R, Rossi M, Mondini AC, Santurri L, Ardizzone F, Guzzetti F. 2011. Seasonal landslide mapping and estimation of landslide mobilization rates using aerial and satellite images. Geomorphology 129:59-70.

Greenway DR. 1987. Vegetation and slope stability. In: Anderson MG and Richards KS, editors Slope stability. New York. ST: J Wiley ＆Sons.

Horvitz CC, Pascarella JB, McMann S, Freedman A, Hofestetter RH. 1998. Functional roles of invasive non-indigenous plants in hurricane-affected subtropical hardwood forests. Ecol Appl 8(4):947-74.

Hsieh SC, Chen WP, Lin WC, Chou FS, Lai JR. 2012. A study of the application of an average energy entropy method for the endpoint extraction of frog croak syllables. Taiwan J For Sci 27(2):177-89.

Huang TC. 2003. Flora of Taiwan, 2nd ed. Vol.

6. Taipei Taiwan: Department of Botany, National Taiwan Univ.
Huang YL, Chen SJ, Kao WY. 2012. Floral biology of *Bidens pilosa* var. *radiata*, an invasive plant in Taiwan. Bot Stud 53(4):501-7.
Huang YL, Kao WY. 2014. Different breeding systems of three varieties of *Bidens pilosa* in Taiwan. Weed Res 54:162-8.
Kasai M, Ikeda M, Asahina T, Fujisawa K. 2009. LiDAR-derived DEM evaluation of deep-seated landslides in a steep and rocky region of Japan. Geomorphology 113:57-69.
Lin DG, Chiou BJ, Wang SH, Lin SH. 2013. 3-D mechanical conversion model for the soil-root system of the predominant plant in the Shi-Men watershed. J Chin Soil Water Conserv 44(2):105-20. [in Chinese with English summary].
Lin SH, Hsu HY, Liu WT, Lin DG. 2012. Evaluation of the shear strength increment of the shear strength increment of *Trema orientalis* soil-root system due to roots. J Chin Soil Water Conserv 43(1):43-56. [in Chinese with English summary].
Lu SS, Lin WC, Chen YH, Lin CC. 2009. Application of wireless sensor network to study the defensive behavior of *Apis cerana* (Hymenoptera: Apidae). J Natl Park 19(1):1-8. [in Chinese with English summary].
Lu SY, Lin CY, Hwang LS. 2011. Spatial relationships between landslides and topographical factors at the Liukuei Experimental Forest, southwestern Taiwan after Typhoon Morakot. Taiwan J For Sci 26(4):393-408.
Mackey EC, Tudor GJ. 2000. Land cover changes in Scotland over the past 50 years. In: Alexander R, Millington AC, editors. Vegetation mapping: from patch to planet. New York, ST: J Wiley & Sons.
McKeana J, Roering J. 2004. Objective landslide detection and surface morphology-mapping using high-resolution airborne laser altimetry. Geomorphology 57:331-51.
Odum EP, Odum HT. 1959. Fundamentals of ecology. Philadelphia PA: W.B. Saunders. 400 p.
Santangelo M, Cardinali M, Rossi M, Mondini AC, Guzzetti F. 2010. Remote landslide mapping using laser rangefinder binocular and GPS. Nat Haz Earth Syst Sci 10:2539-46.
Stinson KA, Campbell SA, Powell JR, Wolfe BE, Callaway RM, et al. 2006. Invasive plant suppresses the growth of native tree seedlings by disrupting belowground mutualisms. PLoS Biol 4(5):e140.
Townsend PA, Walsh SJ. 2001. Remote sensing of forested wetlands: application of multitemporal and multispectral satellite imagery to determine plant community composition and structure in southeastern USA. Plant Ecol 157:129-49.
Tsou CY, Feng ZY, Chigira M. 2011. Catastrophic landslide induced by Typhoon Morakot, Shiaolin, Taiwan. Geomorphology 127:166-78.
Whitmore TC. 1989. Canopy gaps and the two major groups of forest trees. Ecology 70(3):536-8.